# MODELING OF MATERIAL RESPONSE DURING FIBER DRAWING OF SEMICRYSTALLINE PET

A Thesis

by

SEEMANT YADAV

Submitted to the Office of Graduate Studies of
Texas A&M University
in partial fulfillment of the requirements for the degree of

MASTER OF SCIENCE

May 2006

Major Subject: Mechanical Engineering

# MODELING OF MATERIAL RESPONSE DURING FIBER DRAWING OF SEMICRYSTALLINE PET

A Thesis

by

SEEMANT YADAV

Submitted to the Office of Graduate Studies of
Texas A&M University
in partial fulfillment of the requirements for the degree of

MASTER OF SCIENCE

Approved by:

| | |
|---|---|
| Chair of Committee, | Arun Srinivasa |
| Committee Members, | Ibrahim Karaman |
| | Lee L. Lowery, Jr |
| Head of Department, | Dennis O'Neal |

May 2006

Major Subject: Mechanical Engineering

# ABSTRACT

Modeling of Material Response during Fiber Drawing of Semicrystalline PET. (May 2006)

Seemant Yadav, B.E., Shri Govindram Seksaria Institute of Technology and Science, Indore, India

Chair of Advisory Committee: Dr. Arun Srinivasa

Accurate constitutive modeling of polymeric fibers presents a difficult and distinct challenge. While significant progress has been made in constructing models applicable for small strains and limited strain-rate and temperature regimes, much less has been made for more general conditions. This is due in part to the complexity of polymeric behavior. In this work, experimental results of uniaxial extension tests on Polyethylene terephthalate (PET) were obtained from Dr. S.Bechtel, were analyzed, and were formulated into a new model which explains the behavior of PET at different temperatures and strains. The biggest impediment in the determining the behavior of polymeric was the difference in the behavior of PET above and below its glass transition temperature. Consequently, well established (from microstructural considerations) constitutive models and concepts for rubber elasticity and plasticity were not directly transferable to modeling PET fibers. In the model, the PET fibers were assumed to be constituted by amorphous and crystallization segments and the response of the material during stretching was the combined response of simultaneous stretching of the amorphous and the

crystalline segments. The strengthening mechanism is due to orientation of the amorphous segments during stretching. The model involves a friction element which took account of the plastic behavior below the glass transition temperature. The model was used to predict the response of PET at different temperatures and the results from the model showed good agreement with the experimental data. The results from the research will be further used to increase the overall efficiency of the fiber drawing process.

To

My parents and loving brother

# ACKNOWLEDGEMENTS

I would like to take this opportunity to offer my heartfelt thanks to a number of people without whose help and support this thesis would have never been possible. I must start with my advisor Dr. Arun Srinivasa, for providing me with an opportunity to work with him. He has always guided me through my work and at the same time, given me enough freedom to learn and produce original ideas. He has been the "*Real Inspiration*" behind this work.

My parents have provided me with countless opportunities for which I am extremely grateful. The love that my brother and I share in my life is invaluable to me. Nothing I say here can do justice to the continuous and unending support I get from my family. I must also thank a few friends who have been with me through the ups and downs in my life. Thank you very much Houng, Anshul and Aditya.

I would also like to thank all my teachers who have provided me with adequate knowledge and the power of logical thinking, without which I would have never finished this work.

Last but not the least it gives me immense pleasure to thank the numerous friends who have come in my life at various stages to make it wonderful. Thank you Ajish, Kirti, Tejaswi, Nanda and Praveen. Special thanks to Beka.

# TABLE OF CONTENTS

Page

Page

# LIST OF FIGURES

Page

Page

# CHAPTER I

# INTRODUCTION AND LITERATURE REVIEW

## 1.1 Fiber Drawing: Introduction

Polymeric Fiber drawing is an important industrial process. Drawn fibers are used to make things like textiles and rope. The objective behind drawing fibers is to induce molecular orientation in the fiber, thereby increasing their strength in the direction of the stretch. Draw enhanced morphology and micro-structure is responsible for improved properties of fibers and films [1–6]. Once the fibers have been stretched, or drawn, they are strong enough to make various textile products like polyester. Fiber drawing consists of first spinning the molten polymer into filaments through a capillary and then uniaxially drawing the solidified filaments. The orientation of the polymer molecules can be increased after the spinning process by a subsequent drawing process, in which the solidified, as spun fiber is heated to a temperature above the glass transition temperature and drawn with a series of rollers. The purpose of the draw process is to convert relatively weak as-spun fibers to fibers with greater molecular orientation and the resulting greater strength. This process of spinning is designed to produce a filament with a desired strength, accomplished by inducing sufficient orientation of the polymer molecules along the axial direction of the filament [1].

---

This thesis follows the style and format of the journal Polymer.

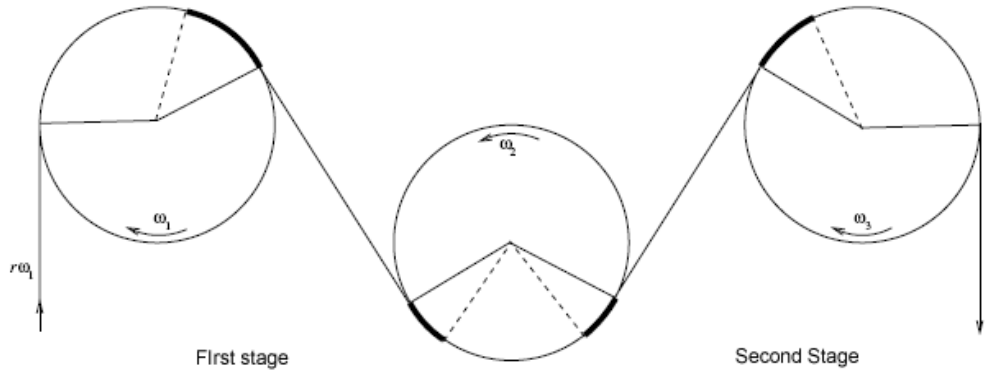


Fig. 1. A typical two-stage draw process [1].

The drawing process of a fiber involves passing the fiber tow over a series of rollers (Fig. 1). The rollers rotate at specified constant angular velocities, each faster than the other. A drawing process can either involve a continuous filament yarn or a staple tow. In some processes all the draw is introduced in one step, in a single stage of feed and take-up rollers. This single draw can result in fiber breakage so it is customary to involve more than one draw processes in the industries. Bechtel et al. [1-3] gave a model for a two-stage draw process in which most of the draw was provided in the first stage (between 2.2 and 2.7 draw ratio) and a relatively smaller draw (1.1-1.2). As the number of stages is increased, it is possible to keep each freespan and roller at a different temperature and induce the maximum possible draw in each stage in order to obtain the maximum molecular orientation in the fiber. Sussmann (as referenced in [1]) introduced the concept of an “Incremental Draw Process”, in which the fiber is drawn on a single pair of shaped rolls through

a large number of small draw increments within a compact space. Draw zone length and residence time are increased substantially, allowing time for morphological change. Production of ultra-orientation, improved tensile modules, high tenacity, low break elongation, and low boil-off shrinkage was reported.

World man-made fiber production in 2004 was up by 8.9% to 34.6 million tons following a 5.2% rise in 2003[7]. The rise in 2003 was slower than the 4.9% increase recorded for 2002 but was in line with average growth rates for the 1990s. Man-made fiber output rose by 4.9% and its share of the total rose from 54.5% to 55.8%. Output of man-made filament rose by 5.3% to 18.9 million tons, which was faster than the 1.4% rise in staple fibers (natural and man-made). Overall, polyester (filament and staple) achieved the fastest growth as output rose by 7.2% to 22.26 million tons—63% of the man-made fiber total. Over 17,000kt (>35 billion pounds) of polyester fiber are produced each year, making it the most widely used fiber in the world [7]. Its commercial dominance is due to a unique blend of high performance, low cost and benign impact on the environment. [8]. The US currently accounts for about 23% of the manufactured polymeric fiber and about 15% of the total fiber consumption.

A detailed economic examination of the processing of fibers and the changes that have taken place during the last half century show two vivid occurrences. The first of these is the rapid decrease in the prices of newer fibers as they became

established, followed by leveling out and stabilization. The second is the relative stability of prices of the manufactured fibers on short term and even long term bases as compared to the fluctuations in the prices for the natural fibers where governmentally imposed stability has not been in effect.

The properties of a fiber have been shown to be highly dependent on the temperature at which it is processed [4-6]. There has been a detailed documentation on the fiber drawing process [1-3]. Below the glass transition temperature ($T_g$), the polymer behaves inelastically and yields plastically with dissipation of energy through internal friction and above the glass transition temperature, it behaves as a rubber. Bechtel et al [1] have proposed a theoretical framework to predict the thermo-mechanical behavior of the fibers during drawing. They assumed that the processing is done at high speeds, allowing little time for viscoelastic effects to occur, so that viscoelasticity can be neglected without resulting in significant errors. The fiber undergoes plastic deformation below $T_g$ and elastic deformation above it. Orientation of molecular segments occurs with initial stretching and with increasing stretch of the fiber crystallization happens, changing the morphology of the fiber. . Argon [6], Ward proposed a theory for the low-temperature plastic deformation of glassy polymers in which he considered the yielding of glassy polymers as a thermally-activated production of local molecular kinks. A large number of models exist which model the fiber above the Glass transition temperature. Boyce and Arruda [5], Makradi [9] have proposed models that explain the working of the

polymer above its Glass transition temperature. Buckley [4] proposed a constitutive model which explains the phenomenon considering two kinds of mechanisms: perturbation of interatomic potentials and perturbation of configurational entropy through a change of molecular conformations.

Rajagopal, Kannan and Rao [10] used a general thermodynamic framework for materials with multiple natural configurations to study the problem of fiber spinning in PET which is amorphous below the glass transition temperature. They propose a form for the rate of entropy production associated with mechanical working and the Helmholtz potential, defined with respect to these evolving natural configurations.

### 1.2 Motivation

The polymer that we are interested in is Poly (ethylene terephthalate) (PET). PET is a polymer of great commercial significance, and while it finds its major uses in fiber, film and bottle applications, there are injection molding uses also. The usages of PET in fibers and films are based on the mechanical orientation of supercooled PET and subsequent heat treatment [5], [11], [12]. Because it provides an excellent barrier against oxygen and carbon dioxide, PET has become a material of choice for bottling beverages, such as mineral water and carbonated soft drinks. It also is used for microwave food trays and food packaging films. But PET is most useful commercially in the form of fibers and films which have a high degree of orientation [5].

Owing to complexities of the dependencies of the material behavior and the complexities of the process itself, it is difficult to experimentally isolate and determine the magnitude of the effects that small variations in different process parameters can have on the end product. Accurate numerical modeling of the process using a technique such as the finite element method could provide valuable insight into the physics of the process and dependencies on various process parameters. In order to conduct such numerical studies, an accurate constitutive model of PET behavior is required. There is a huge demand of polymeric fibers in the world market which adds on the benefits that can be reaped from an efficient model for polymeric fiber drawing [13]. Thus, study and modeling of PET in different conditions poses an interesting problem and this is the problem which has motivated this work.

# CHAPTER II

# PHYSICAL STRUCTURE OF SEMICRYSTALLINE FIBERS

## 2.1 Fiber Structure

When cooled from the melt many polymeric fibers form a disordered structure called amorphous state. Some of these materials, such as polmethyl methacryalate, polystyrene and rapidly cooled (melt-quenched) polyethylene terephthalate (PET), have comparatively high modulus at room temperature, but others, such as natural rubber, have a low modulus [14]. These two types of polymers are often termed *glassy* and *rubber-like* respectively. The behavior of a polymeric fiber depends on the temperature relative to its glass transition temperature ($T_g$). The glass transition temperature of a polymer is dependent on the material. Its precise value depends slightly on the rate of cooling, being lower for lower rates of cooling. The usual cooling rate in observations is 1 $^oC$/min [15]. The fiber behaves as rubber above $T_g$ and as glassy below $T_g$.

A semicrystalline polymer contains a mixture of amorphous and crystalline regions (Fig. 3) [16] Polymer crystallanity is the packing of molecular chains so as to produce an ordered atomic array. Any chain disorder or misalignment will result in an amorphous region. The ratio of the crystalline and amorphous depends on the process. Typically if the polymer is solidified very slowly from the melt the

crystalline part is more than the amorphous part and if the polymer melt is quenched the amorphous part is more than that the crystalline part.

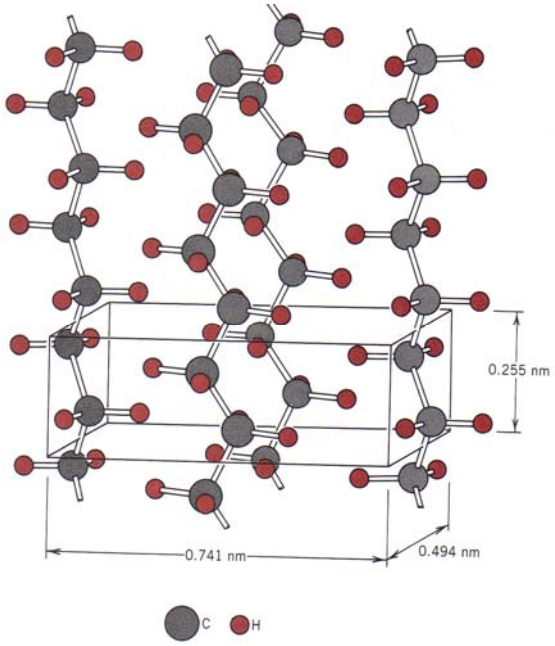


Fig. 2. Arrangement of molecular chains in a unit cell of a polymer [14].

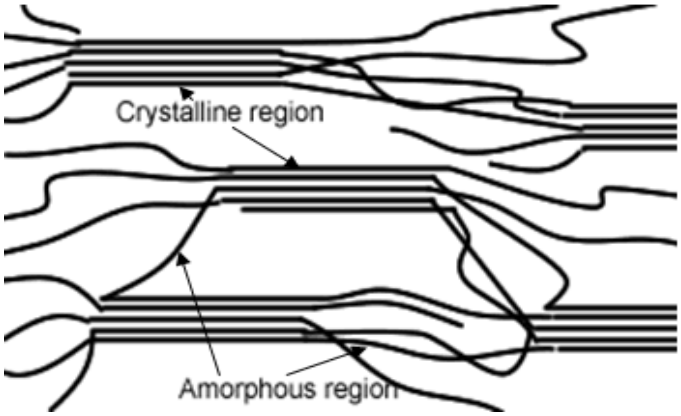


Fig. 3. Structure of a semicrystalline polymer.

In an **amorphous polymer** the molecules are oriented randomly and are intertwined, much like cooked spaghetti, and the polymer has a glasslike, transparent appearance. In semicrystalline polymers, the molecules pack together in ordered regions called **crystallites**, as shown in Fig. 2. As might be expected, linear polymers, having a very regular structure, are more likely to be semicrystalline. Semicrystalline polymers tend to form very tough plastics because of the strong intermolecular forces associated with close chain packing in the crystallites. Also, because the crystallites scatter light, they are more opaque. Crystallinity may be induced by stretching polymers in order to align the molecules. Crystallization induced due to stress and strain has been studied in detail [17], [18], [19]. In the plastics industry, polymer films are commonly drawn to increase the film strength [15].

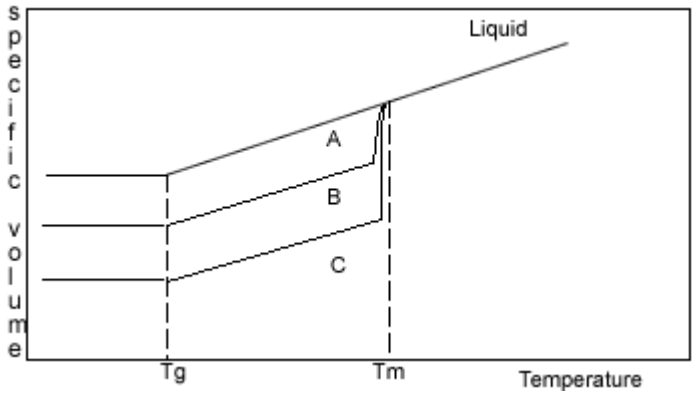


Fig. 4. Specific volume vs. temperature, upon cooling from a liquid melt, for totally amorphous (curve A), semicrystalline (curve B) and crystalline (curve C) polymers.

## 2.2 Temperature Dependence of Polymeric Fibers

At low temperatures, in the glassy state**,** the molecules of an amorphous or semicrystalline polymer vibrate at low energy, so that they are essentially frozen into a solid. As the polymer is heated, however, the molecules vibrate more energetically, until a transition occurs from the glassy state to the rubbery state. The onset of the rubbery state is indicated by a marked increase in volume, caused by the increased molecular motion (Fig. 4). The point at which this occurs is called the glass transition temperature [14]. The polymer that we are interested in, Poly(ethylene terephthalate) (PET), has a glass transition temperature is 79 deg C. In the rubbery state above $T_g$, polymers demonstrate elasticity, and some can even be molded into permanent shapes. One major difference between plastics and rubbers, or elastomers, is that the glass transition temperature of rubbers is below room temperature—hence their well-known elasticity at normal temperatures. Plastics, on the other hand, must be heated to the glass transition temperature or above before they can be molded.

When brought to still higher temperatures, polymer molecules eventually begin to flow past one another. The polymer reaches its melting temperature ($T_m$ in the phase diagram) and becomes molten (progressing along the line from *c* to *d*). In the molten state polymers can be spun into fibers. Polymers that can be melted are called thermoplastic polymers. Thermoplasticity is found in linear and branched polymers, whose looser structures permit molecules to move past one another. The

network structure, however, precludes the possibility of molecular flow, so that network polymers do not melt. Instead, they break down upon reheating. Such polymers are said to be thermosetting [14].

All the polymers consist of chemical and physical crosslinks through which they are attached to other molecules. The crosslinks are of two types: *Primary* and *Secondary*.

Primary crosslinks are those which are formed in the process of the polymerization of the polymer. Primary crosslinks do not break during deformation so that they are permanent. Secondary crosslinks on the other hand are those which are formed by H-bonded carboxyl groups. Even in equilibrium the H-bonds are constantly breaking and reforming. The amount of H-bonds depends on the temperature [20] (Figs. 5 and 6).

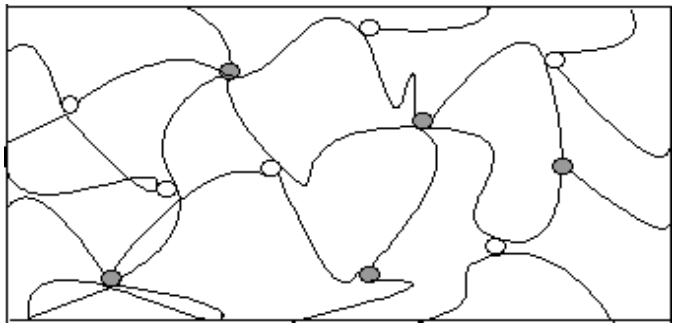

Fig. 5. Deformed network showing primary (●) and secondary (o) bonds below glass transition temperature**.**

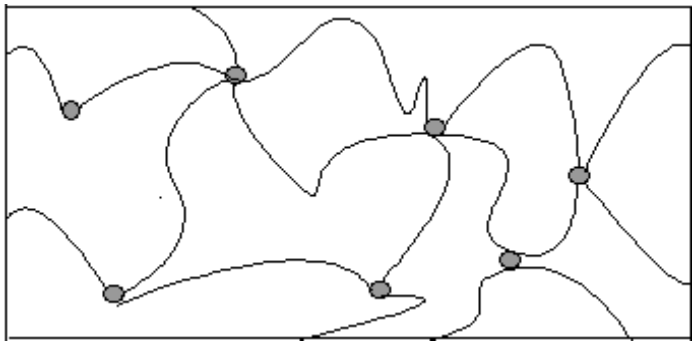

Fig. 6. Deformed network showing primary (●) and secondary (o) bonds above glass transition temperature[20].

At temperatures below $T_g$, the secondary bonds break due to stretching of the polymeric fiber. The primary bonds get displaced in an affine manner. But at temperatures above $T_g$, the molecules have enough thermal energy to break the secondary bonds and the wriggling motions of the fiber chain segments become easier. This distinct form of motion is often termed as *reptation*. Since the covalent bonds connecting each atom within a molecule can now rotate and bend easily, a single molecule can take on numerous conformations and hence has high configurational entropy. A process such as stretching of a fiber decreases its entropy. Thus, the large retractive force in fibers above their $T_g$ are induced by a change in entropy. On the other hand below $T_g$, the conformation changes are not possible because of the secondary bonds. Thus entropic changes are not the main cause of the reactive forces. The reactive forces are produced by the stretching of the bonds. Hence the stiffness increases. Moreover, if sufficient force is applied to change in configuration, this configuration remains and the material does not

recover its original configuration when the forces are removed. This is the reason for the possibility of molecular alignment by stretching.

The stretched polymer upon heating above $T_g$ will recover it original shape. This behavior of the polymer is the reason behind its shape memory effect [21].

# CHAPTER III

# DEFORMATION OF SEMICRYSTALLINE POLYMERS

## 3.1 Deformation Mechanisms in Semicrystalline Polymers

Most of the semicrystalline polymers have the spherulitic structure, which consists of mixture of amorphous and crystalline segment. A semicrystalline polymer deforms in the following steps

- elongation of amorphous tie chains
- tilting of lamellar chain folds towards the tensile direction
- separation of crystalline block segments
- orientation of segments and tie chains in the tensile direction

The mechanisms of deformation of a semicrystalline polymer vary depending on its temperature. Below the $T_g$, the polymeric fiber undergoes inelastic deformation which is characterized by yielding. Below $T_g$ the molecules form a sluggish mixture of amorphous and crystalline regions. The chain backbone configurations are largely immobilized. So when a semicrystalline polymer is stretched, the distance between the tie chains increase but their configuration remains unaltered. The molecules align preferentially along the stretch direction (Fig. 5). During the initial stage of deformation, the lamellar ribbons simply glide past one another as the tie chains within the amorphous regions become extended. Continued deformation in the second stage occurs by the tilting of the lamellae so that the chain folds become

aligned to the tensile axis. Next, crystalline blocks segments separate from the lamellae, which segments remain attached to one another by tie chains. In the final stage the blocks and the tie chains become oriented in the direction of the tensile axis. Thus appreciable tensile deformation of semicrystalline produces highly oriented structure.

The final fiber morphology not only depends on the final state of strain induced by the process, it also depends on the thermodynamic path experienced by the fiber while reaching that final state. The information on the real-time evolution of fiber morphology can be extracted by studying its development using in-situ measurements, particularly using high brilliance synchrotron X-rays. It has been noticed that for crystallization during the spinning process, small angle x-ray scattering (SAXS) intensity increases prior to wide-angle x-ray diffraction (WAXD), thus a combination of SAXS and WAXD can be applied to characterize the morphology development in fibers [17]

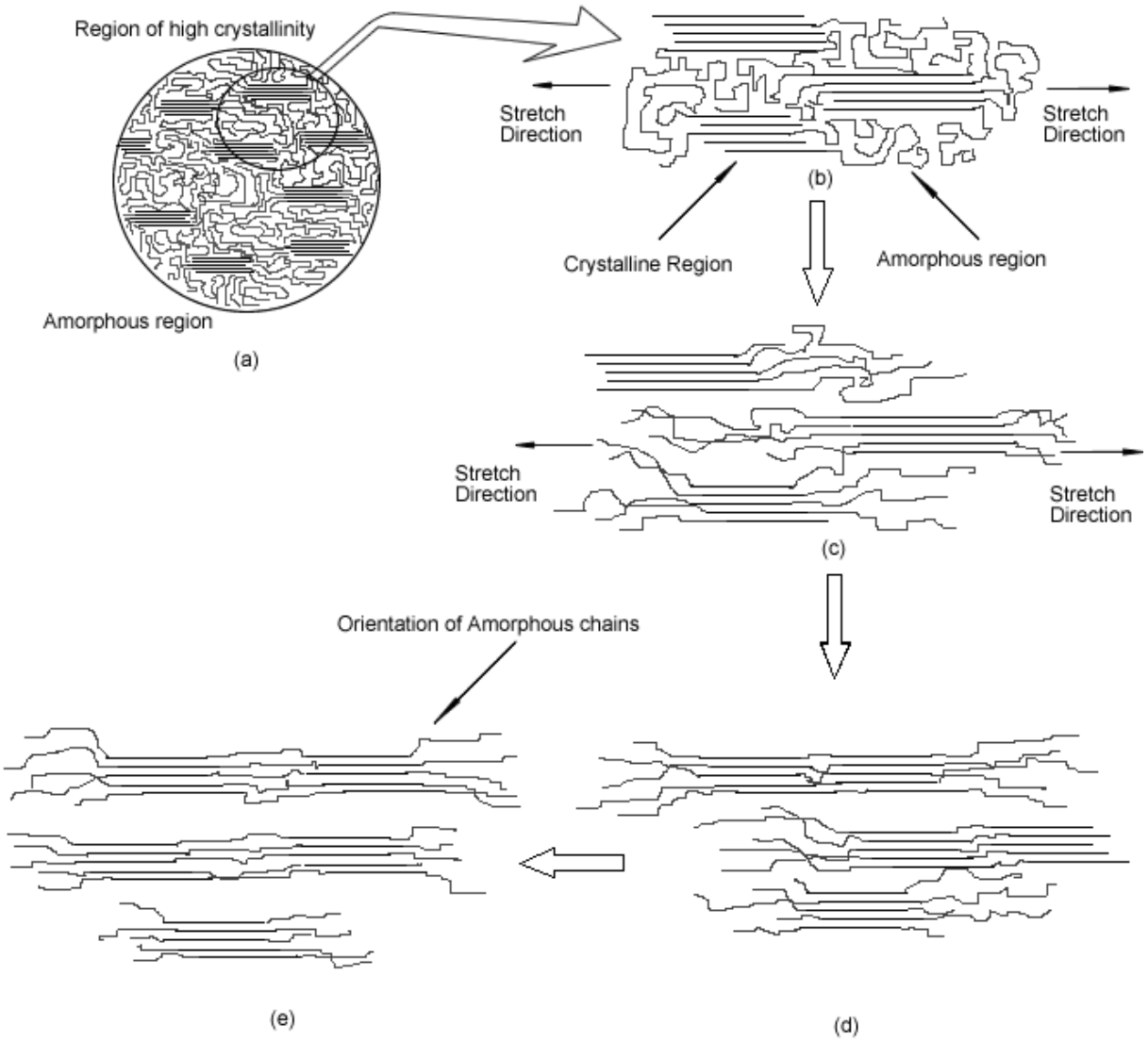


Fig. 7. Stages in the deformation of a semicrystalline polymer. (a) Fringed-michelle model of a semicrystalline polymer, showing both the crystalline and amorphous regions (b) Enlarged view of a section in the polymer (c) Elongation of amorphous tie chains during final deformation

Various studies on SAXS and WAXD have been done by Chaouche and co-workers [22]. In their work, Chaouche and co-workers have concluded that at small draw ratios there is no measurable crystallinity. In this region, the polymer would be in an uncross-linked state. This is followed by some kind of a plateau during which oriented nuclei would develop. The last part of the stress-strain curve corresponds to the crystallization growth.

This orientation of the structure is different from crystallization (Fig. 7). The molecules are merely aligned in one direction unlike crystallization where they form a regular, repeated structure in a uniform manner. Boyce et al [5] have used the change in crystallization as the basis of the strain hardening phenomenon observed during the plastic deformation of polymeric fibers. Recent studies by Gorlier et al.[18] (Fig. 8) have shown that crystallization ratio is not the accurate parameter to be introduced in models for a constitutive equation for PET even if, in certain case some sets of experiments enable to draw empirical relationships between these two parameters. Hence in the present work, the basis for strain hardening is taken to be orientation of the polymeric fibers and not the crystallization of the fibers. For lower strains, it is the orientation leads to the initial strain hardening of the polymeric fiber.

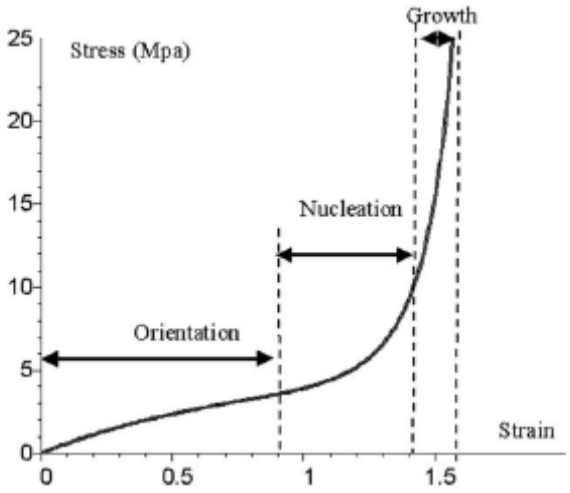


Fig. 8. Schematic kinetics of microstructure development of PET [14].

### 3.2 Yielding in Polymers

After a certain strain, below $T_g$, yielding occurs. Macroscopically the phenomenon of yielding in polymeric fiber looks similar to yielding in metals but at a molecular level the two phenomena are dissimilar. Yielding in polymeric fiber is the result of slippage of lamellae and breaking of secondary bonds, unlike movements of dislocations as in metals. Yielding in polymeric fibers is a function of temperature entire strain history up to and including the yield point [23]. Fig. 9 shows the effect of increase in temperature on yield stress of PET. The graph was plotted from experimental results obtained by Ward and co-workers. The ratio of change in yield stress in the experiments done by Bechtel et al matches these experimental results (a ratio of 3). Unlike metals, there is no necking in polymeric fibers on further stretching. There is no yielding in a polymeric fiber above the $T_g$ since molecular segments have enough thermal energy to move past one another. So, it is easier for

the molecular segments to change their conformation than slippage of lamellae. There is a drop in the load after yielding. This drop in load is attributed to an intrinsic yielding process [24]. Brown and Ward [24] demonstrated that localized heating during stretching causes softening and hence reduction in the load.

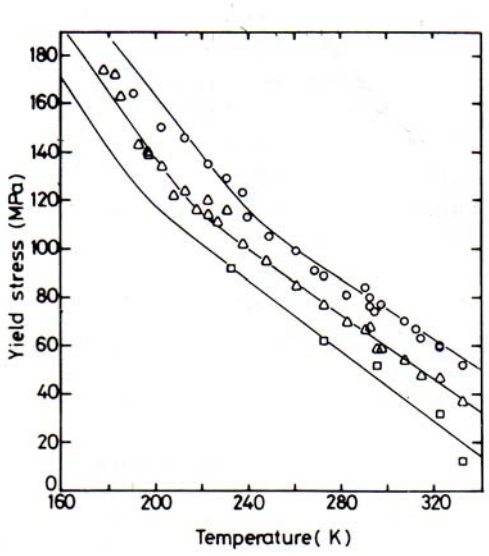


Fig. 9. Variation of yield stress of PET with temperature [24]

The effect of increase of temperature on Elastic Modulus (E) of the fiber is similar to that on yielding. Fig. 10 shows the effect of increase in temperature on the elastic modulus of PET. E falls considerably around $T_g$. Since we are neglecting the viscoelastic effects in the modeling procedure, we neglect the effect of time of the elastic modulus for the purpose of modeling. The softening of the fibers around $T_g$ can again be explained on the similar terms as yielding. Polymeric fiber chains which are less energetic (more sluggish) are also more reluctant to move under a

force. This makes it more difficult for them to unfold, so that their ability to undergo large deformations is suppressed. In this state, polymeric fibers are more likely to resist the applied load and are, therefore, stiffer.

At higher temperatures, the energy level of chains favors their movement, so unfolding is easier. In contrast to lower temperatures, a given amount of deformation requires a lower force and, by the same token, a force of a given magnitude produces a larger deformation.

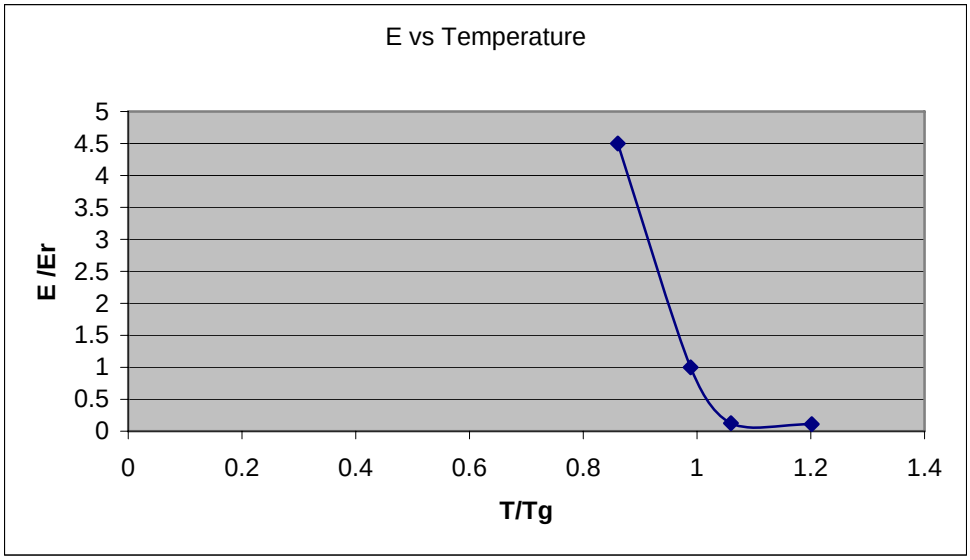


Fig. 10. Variation of modulus with temperature for PET.

# CHAPTER IV

# EXPERIMENTAL RESULTS

## 4.1 Experimental Results

The experiments were done at the Ohio State University, Columbus Ohio by Dr. S.E Bechtel. The following were the results that were obtained from these experiments.

Differential Scanning Calorimetry (DSC) tests were performed on the samples and following were the results.

### 4.2.1 Glass Transition Temperature

Tg was measured by DSC, Model TA 2920. Tg of the fiber is 79 °C according to our experiment (2 times). The valley and peak in Figs. 11 and 12 is believed to be caused by processing process and the peak region shows cold crystallization.

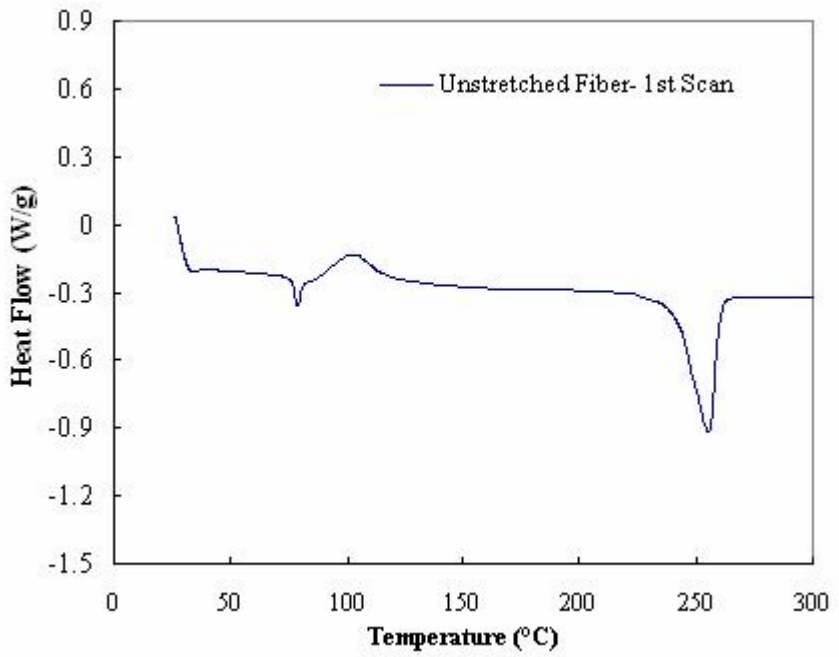


Fig. 11. DSC results for unstretched fiber.

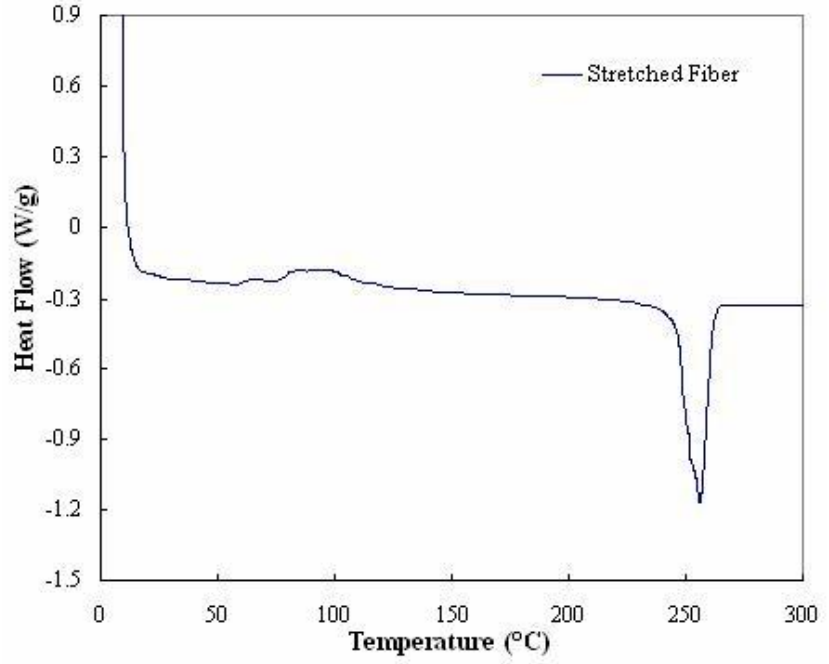


Fig. 12. DSC results for stretched fiber.

### 4.1.2 Melting Point

Tm was also measured by DSC. Tm is 256.36°C according to 5 tests.

The Tg of PET fiber is usually in the range of 75°C and the melting temperature is 260°C. So the Tg and Tm of the fiber we have, agree with the properties of PET fiber.

### 4.1.3 Crystallinity

Crystallinity was calculated as follows:

$$Crystallinity\% = \frac{Hm - Hc}{H_m^o} \times 100\%$$

where Hm is the heat of melting, Hc is the heat of the cold crystallization, and $Hm^o$ is the heat of pure crystalline polymer. The $Hm^o$ of PET is 140.1 J/g from the literature.

The stretching speed was 0.1 mm/s for all samples and the final extension is 70%. Please note that 20% and 40% extension lie in *soft plateau* region, while 53% and 70% extension are in stiff region after the plateau. Average crystallinity of two measurements is reported in Table 1.

Table 1 Comparison of % Extension with % Crystallinity

| Extension (%) | 0% | 2% | 20% | 40% | 53% | 70% |
|---|---|---|---|---|---|---|
| Crystallinity (%) | 25.% | 26.0% | 26.6% | 28.2% | 29.6% | 32.8% |

### 4.1.4 Stress Strain Curve

*High strain tension test at a low stretching speed*

The high strain tension test was re-conducted at a very low stretching speed, 0.04 mm/s. The total time of the stretching process is 41.5 minutes. The final extension is 70%. The previous high-speed tension test was performed at the stretching speed of 0.2 mm/s. The results are shown in Fig. 13. It was found that unloading and reloading process are the same at different stretching speeds. However, some difference can be found as follows:

a. The transition from low linear strain region to the soft plateau is not sharp any more. A curvature can be found at the transition at the low stretching speed. It means overshot is not severe.
b. The load is a little bit lower at a low stretching speed than at a high stretching speed.
c. The slope at the stiff region is much smaller at a low stretching speed than a high stretching speed.

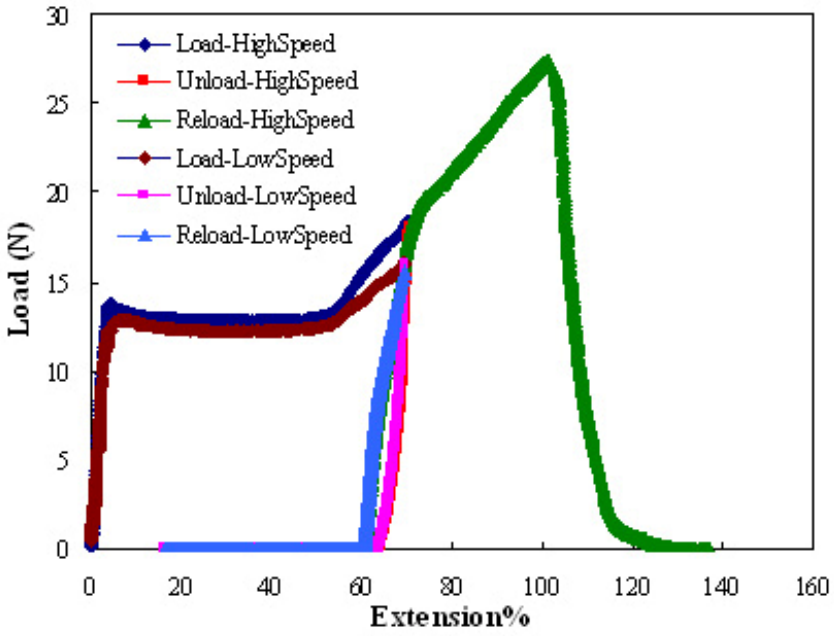


Fig. 13. Stress-strain curve for PET.

The absence of the sharp upper yield point shows that yield point might be dependent on the speed of straining. Also, the hardening due to orientation is lesser at low speed than hardening due to orientation ay high speed. Thus, orientation is a function of strain rate as well as temperature. The model is developed with at a strain rate of 0.02mm/s.

# CHAPTER V

# MODEL FORMULATION

## 5.1 Model Description

The present work follows closely the work of Kratochv´ıl, Rajagopal, Srinivasa and M´alek [25]. Kratochv´ıl et al modeled the response of an elasto-plastic material as a result of response of hard and soft regions. They took into consideration the changes in microstructure during plastic deformation. The soft phase was assumed to be non-hardening while the hardening response of the hard phase was assumed to be dependent upon the response of both the hard and soft phases. The material was supposed to have multiple natural states and the response of the material from these states is elastic. When, the material is deformed, it's underlying natural state changes, thus leading to a corresponding change in the response function. The dissipation was associated with the change in the natural configuration of the material.

In the model, the material is assumed to be a mixture of a crystalline phase and amorphous phase. The resistance due the amorphous and the crystalline regions are treated separately. It is assumed to be isotropic before stretching. The initial crystallinity was found out to be 25.7% and the final crystallinity was found to be 32.8% through the experiments. An increase of 8.1% did not account for a large

strain hardening. This result was substantiated by experimental results by Gorlier et al [18], in which they showed that crystallization does not take place until the strain developed is more than 100%. Fig. 14 shows the results of the work by Gorlier and co-workers. It clearly shows that for strains less than 100% the only orientation of fibers occurs and since during fiber drawing process the strain induced in any stage is less than 100%, therefore in the model, we attribute strain hardening to the segmental orientation rather than crystallization.

The specimen used was an ultra thin fiber of area of cross section $1mm^2$. There was no observed necking in the fiber. Von-Mises criteria was assumed for yielding [26].

**5.2 Model Features**

Following are the salient features of the model.

1. The material is assumed to be a mixture of crystalline and amorphous segments.
2. The elastic response is due to the deformation of the laminae and the stretching of the secondary bonds with no significant changes in the conformation and hence entropic elasticity is negligible [14].
3. Below $T_g$, plastic deformation occurs due to the molecular alignment. Hence the plastic strain itself is a measure of the degree of alignment.

4. Since molecular alignment does not continue indefinitely, there is a maximum amount of plastic strain that is possible. After which the crystallization of segments happens [16].
5. During the process of molecular alignment there is dissipation of energy due to breaking of secondary bonds and slippage of lamellae.
6. Above $T_g$, the thermal energy of the molecules is sufficient to overcome the secondary bonds to cause rapid changes in the conformation. This causes recovery of the aligned molecules (but not of the crystalline phase). Thus, there is no loss of energy.

### 5.3 For Temperature < $T_g$

*Loading*

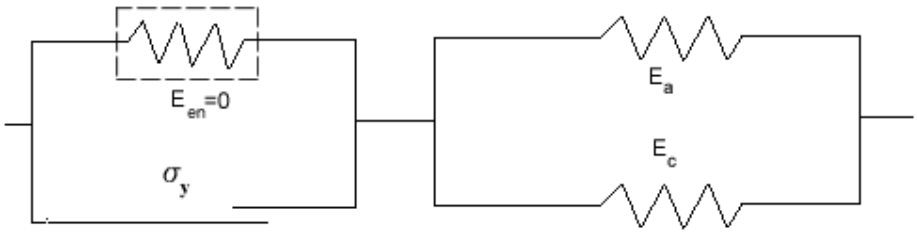


Fig. 14. Model for PET below glass transition temperature

There are two ways of developing stresses in a polymeric fiber. First is by stretching of the bonds and the second is by changing its conformations. Below the glass transition temperature, the polymeric segments do not have enough energy to

rotate and change their conformations. Thus, the only possible way in which the fibers respond to an external stress is by way of stretching. The initial response is due to the stretching of the amorphous and crystalline segments. In the model this response is given by the spring elements (Fig. 14). After a threshold strain, the slipping of the lamellae takes place. In the model this response comes from the friction element. For isothermal processes, the rate of entropy production is governed by the reduced energy equation (Truesdell and Noll [27]).

$$\sigma.\dot{\varepsilon} - \dot{\psi} = \xi \qquad (1)$$

where

$\sigma$ is the Cauchy stress

$\dot{\varepsilon}$ is the total strain rate

$\dot{\psi}$ is the rate of change of Helmholtz potential

$\xi$ is the rate of dissipation of mechanical work.

The friction element develops the irrecoverable plastic strain below the Glass transition temperature. The Helmholtz potential for the model below the Glass transition temperature is given by

Let the strain developed due to bond stretching be $\varepsilon_e$ and the strain developed due to configuration changes of the molecular segments be $\varepsilon_p$.

Assuming that elastic and plastic strains are additive in nature [26]

$$\varepsilon_e = \varepsilon - \varepsilon_p$$

we have

$$\psi = \frac{1}{2} E_{en} {\varepsilon_p}^2 + \frac{1}{2}\left(\bar{E}\right)\left({\varepsilon_e}^2\right) \tag{2}$$

Where $\bar{E} = E_c + E_a$

$$\psi = \frac{1}{2} E_{en} {\varepsilon_p}^2 + \frac{1}{2}\left(\bar{E}\right)\left(\varepsilon - \varepsilon_p\right)^2$$

$$\dot{\psi} = \left(\frac{\partial \psi}{\partial \varepsilon}\right)\dot{\varepsilon} + \left(\frac{\partial \psi}{\partial \varepsilon_p}\right)\dot{\varepsilon}_p \tag{3}$$

Now,

$$\frac{\partial \psi}{\partial \varepsilon} = \left(\bar{E}\right)(\varepsilon - \varepsilon_p) \tag{4}$$

and

$$\frac{\partial \psi}{\partial \varepsilon_p} = E_{en}\varepsilon_p - \left(\bar{E}\right)\left(\varepsilon - \varepsilon_p\right) \tag{5}$$

Thus, we have

$$\frac{\partial \psi}{\partial \varepsilon_p} = E_{en}\varepsilon_p - \bar{E}(\varepsilon - \varepsilon_p)$$

On substituting these values in (2), we get

$$\dot{\psi} = \left\{\bar{E}(\varepsilon - \varepsilon_p)\right\}\dot{\varepsilon} - \left\{E_{en}\varepsilon_p + \bar{E}(\varepsilon - \varepsilon_p)\right\}\dot{\varepsilon}_p \tag{6}$$

Using (1)

$$\sigma.\dot{\varepsilon} - \dot{\psi} = \xi$$

Following Rajagopal and Srinivasa [28], the rate of dissipation is assumed as a constitutive function and a relation for the plastic strain is going to be calculated.

Assuming a form for $\xi$,

$$\xi = \sigma_y \left\|\dot{\varepsilon}_p\right\| \tag{7}$$

From (1), (6), (7) and (8) we have

$$-\left\{E_{en}\varepsilon_p - \bar{E}(\varepsilon - \varepsilon_p)\right\}\dot{\varepsilon}_p = \sigma_y \left\|\dot{\varepsilon}_p\right\| \tag{8}$$

A non-trivial solution for $\dot{\varepsilon}_p$ in (8) is only possible under the following conditions

$$\dot{\varepsilon}_p \begin{cases} = 0 & \sigma < \sigma_y + E_{en}\varepsilon_p \\ \neq 0 & \sigma = \sigma_y + E_{en}\varepsilon_p \end{cases}$$

The yield function can be written as

$$f(\sigma) = \frac{\left\| \sigma - (\sigma_y + E_{en}\varepsilon_p) \right\|}{k} - 1 = 0$$

The yield stress of a polymer is a function of its temperature and strain. Assuming a function of the form

$$\sigma_y = \sigma_{y0}\left(T\right) + \sigma_y\left(\varepsilon_p, T\right) \tag{9}$$

where

$$\sigma_y\left(\varepsilon_p, T\right) = A \times \left[ \frac{\left(\frac{\varepsilon_p}{\varepsilon_0}\right)^n}{1 + \left(\frac{\varepsilon_p}{\varepsilon_0}\right)^n} \right] \times \left( \left(\frac{\varepsilon_p}{\varepsilon_0}\right)^2 - 1 \right)$$

$$A = A\left(T\right)$$

$$n = n\left(T\right)$$

$$\varepsilon_0 = \varepsilon_0\left(T\right)$$

*n* can be chosen to be any value greater than five. For the present case, we chose *n*=27 but any other value of *n* would have given the same answer.

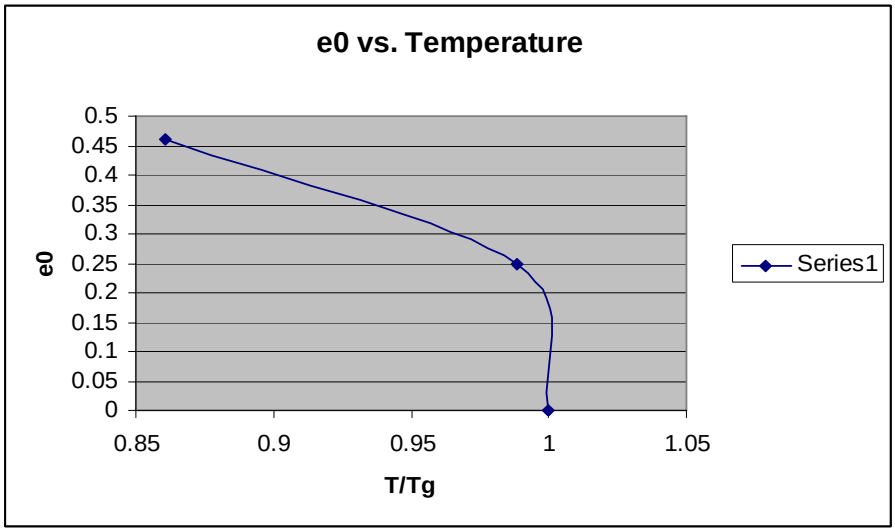


Fig. 15. Variation of e0 with temperature.

$$A(T) = 4000000\left\{\left(\frac{303}{T}\right)^{1/8.092}\right\}\left\{1-\left(\frac{\left(\frac{T}{Tg}\right)^{27}}{1+\left(\frac{T}{Tg}\right)^{27}}\right)\right\}$$

$$\sigma_{y0}(T) = 12200000\left\{\left(\frac{303}{T}\right)^{1/9.664822}\right\}\left\{1-\left(\frac{\left(\frac{T}{Tg}\right)^{27}}{1+\left(\frac{T}{Tg}\right)^{27}}\right)\right\}$$

The variation of e0, A(T) and yield stress with temperature is shown in Figs. 15, 16 and 17 respectively.

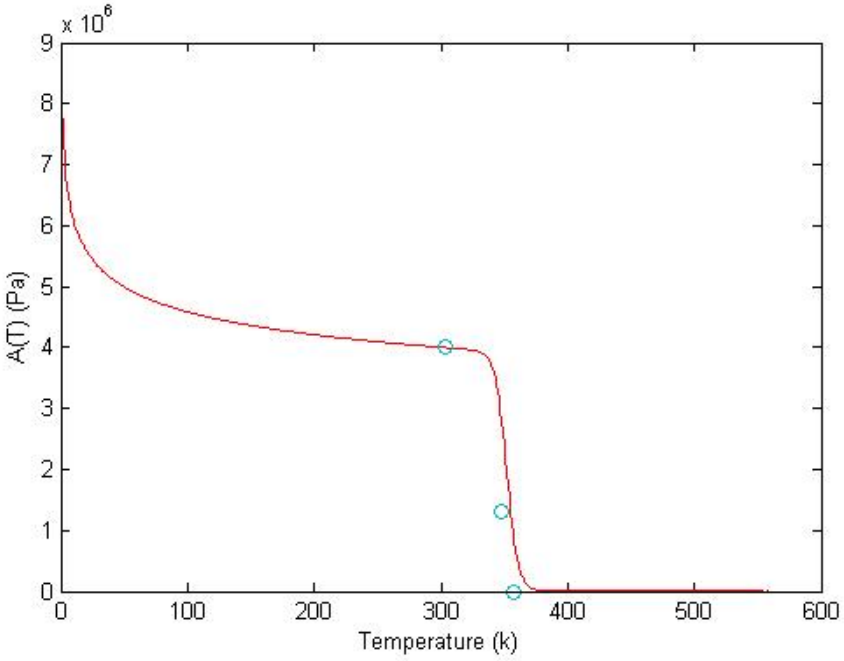


Fig. 16. Variation of A with temperature.

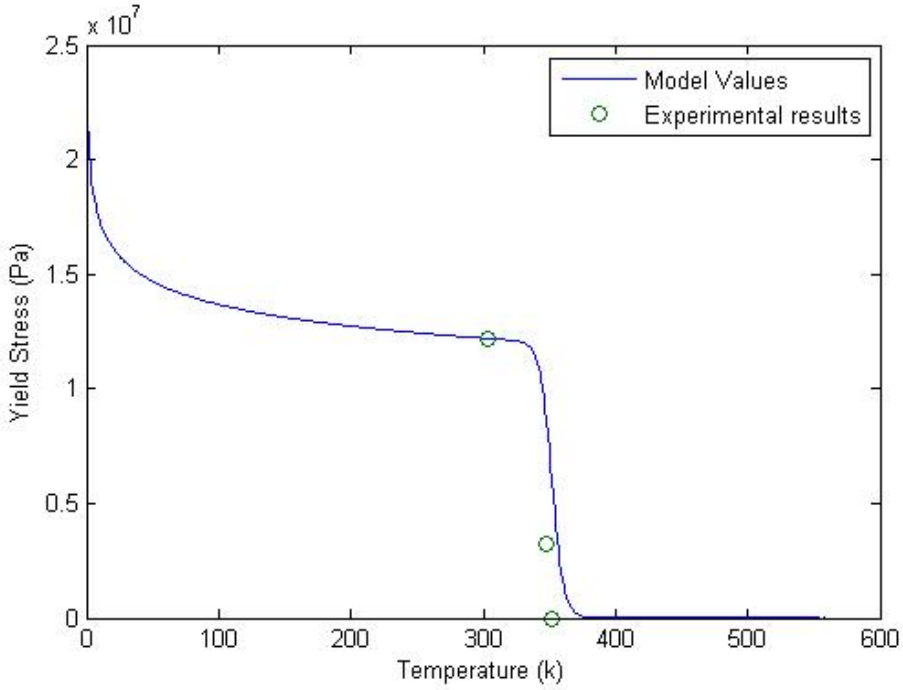


Fig. 17. Variation of yield stress with temperature**.**

*Unloading*

During unloading, the stress decreases and since for unloading the stress will always be less until the material is loaded in the other direction, i.e. compressed. Thus, the material releases any elastic strain it had and when the stress is removed completely, the only strain that remains is because of the changes in configurations of the molecular segments. This strain can be recovered by heating the fiber above its $T_g$. Thus, the strain is not permanent as in metals.

## 5.4 For Temperatures >$T_g$

*Loading*

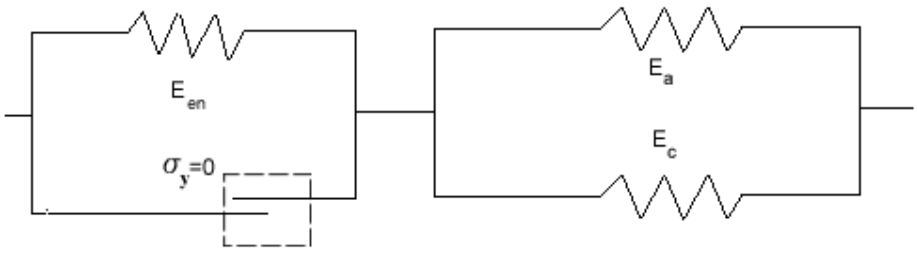


Fig. 18. Model of PET above glass transition temperature.

At temperatures greater than $T_g$ the thermal energy of the molecular segments in enough to change the conformation of the segments. Hence, it is easier for the molecules to rotate than to stretch. Thus there is no sliding of the lamellae takes place and consequently there is no yielding. Thus the effect of the friction element

is completely nullified and the plastic strain is recoverable if the material is heated. The fiber acts as a mixture of elastic amorphous and crystalline segments and thus the response of the fiber is elastic (Fig. 18). The resultant modulus is given by

$$\frac{1}{E_{Total}} = \frac{1}{E_{en}} + \frac{1}{E_c + E_a} \tag{10}$$

where

$E_{en} = E_{en}(\mathrm{T})$

$E_c = E_c(\mathrm{T})$

$E_a = E_a(\mathrm{T})$

The Helmholtz potential (stored energy) is give by

$$\psi_{total} = \psi_1 + \psi_2 \tag{11}$$

where $\psi_1 = \frac{1}{2}\left(E_{en}\right)\varepsilon_p{}^2$

and $\psi_2 = \frac{1}{2}\left(E_c + E_a\right)\varepsilon_e{}^2$

$\varepsilon_e$ and $\varepsilon_p$ are the elastic strains developed due to bond stretching and rotations of bonds respectively.

Thus, from 11 we get

$$\psi = \frac{1}{2}\left(E_{en}\right)\varepsilon_p{}^2 + \frac{1}{2}\left(E_c + E_a\right)\varepsilon_e{}^2$$

and

$$\dot{\psi} = \left(E_{en}\right)\varepsilon_p\dot{\varepsilon}_p + \left(E_c + E_a\right)\varepsilon_e\dot{\varepsilon}_e$$

From equation (7) we have

$$\xi = 0$$

Since $\sigma_y = 0$

On putting this value of $\dot{\psi}_{total}$ in the dissipation equation, we get

$$\sigma.\dot{\varepsilon} - \dot{\psi} = 0$$

or

$$\sigma(\dot{\varepsilon}_p + \dot{\varepsilon}_e) = \left(E_{en}\right)\varepsilon_p\dot{\varepsilon}_p + \left(E_c + E_a\right)\varepsilon_e\dot{\varepsilon}_e$$

which gives

$$\sigma = \left(E_{en}\right)\varepsilon_p = \left(E_c + E_a\right)\varepsilon_e \qquad (12)$$

On solving (12), we get (10), i.e.

$$\frac{1}{E_{Total}} = \frac{1}{E_{en}} + \frac{1}{E_c + E_a}$$

Thus the material behaves as a spring whose modulus is dependent on the temperature.

*Unloading*

The elasticity of the molecular segments above $T_g$ is due to the changes in entropy [15]. The strain induced is completely reversible since molecules have enough thermal energy to recoil back. Thus, the unloading path is the same as the loading path and in the stress-free state there is no strain in the material.

# CHAPTER VI

# RESULTS

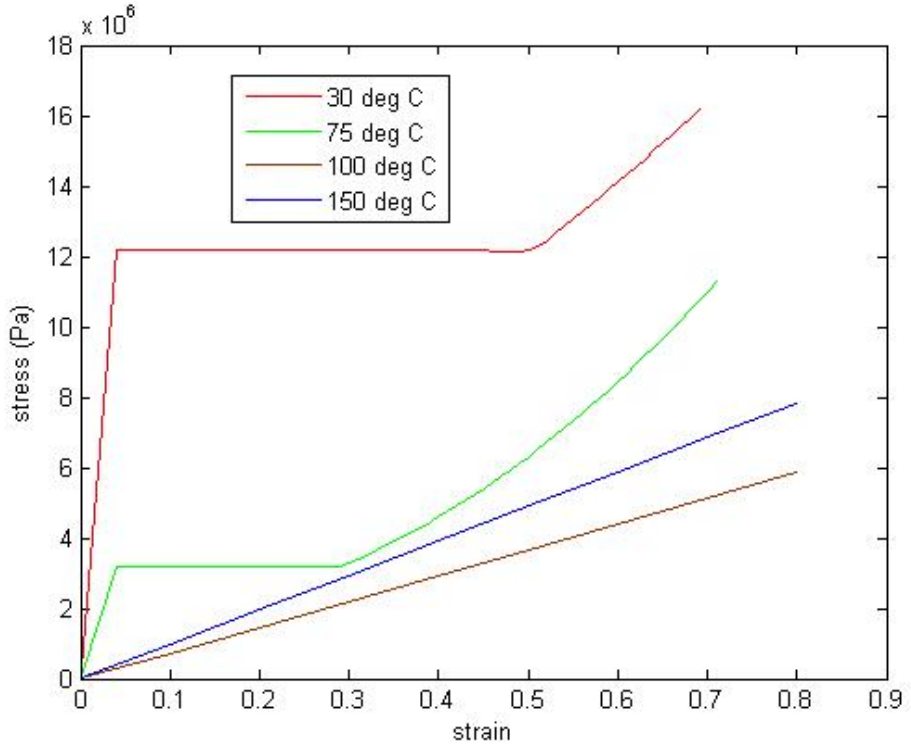


Fig. 19. Model Response at different Temperatures.

Of interest in this section is the predicted behavior of PET by the model. Fig. 19 shows the results obtained from the model. The model depicts the behavior of PET above and below its $T_g$. It shows the strain hardening taking place at higher strains due to orientation of fiber segments. Below $T_g$ it shows irrecoverable strains

developed due to permanent bond stretching. Above $T_g$ the response is rubber-like with full recovery of strains once the applied stress is removed.

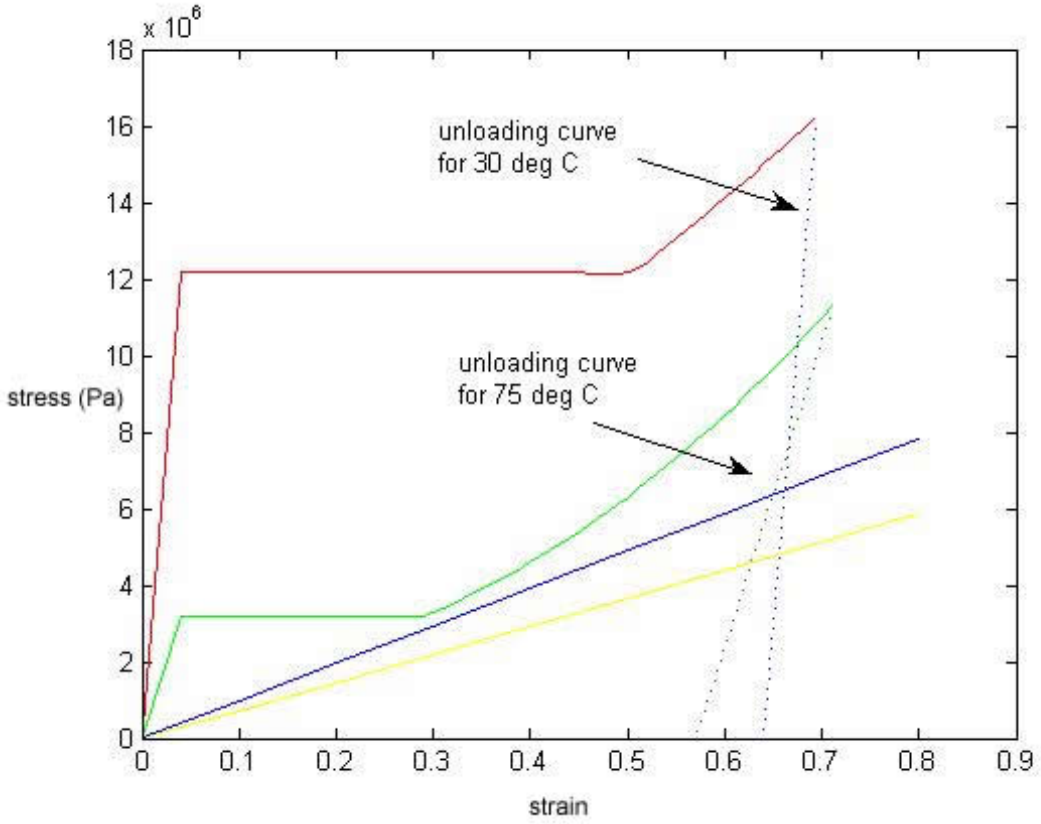


Fig. 20. Model response showing the unloading path.

Fig. 20 shows the unloading curves at 30 ºC and 75 ºC. The unloading paths are approximately parallel to the loading part before yielding. This shows that the once the stresses are completely removed, the only strain left is the irrecoverable strain.

# CHAPTER VII

# CONCLUSION AND FUTURE WORK

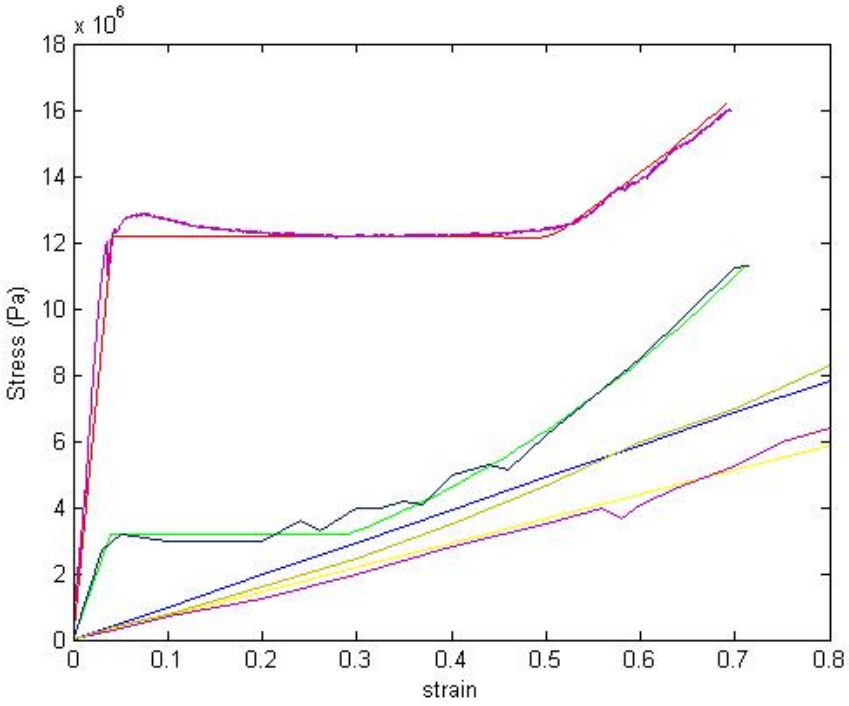


Fig. 21 .Comparison of model response with experimental results.

Fig. 21 shows the comparison of the model results and the experimental data. Results from the model show good agreement with the experimental data. Fig. 22 shows the comparison of a experimental data and the prediction by the model for a process in which the material is first stretched at a constant temperature by a stress of 1.58 MPa and then the temperature was increased keeping the load constant. Fig.

23 shows the comparison of the unloading paths. The unloading path approximated by the model shows good agreement with the experimental results.

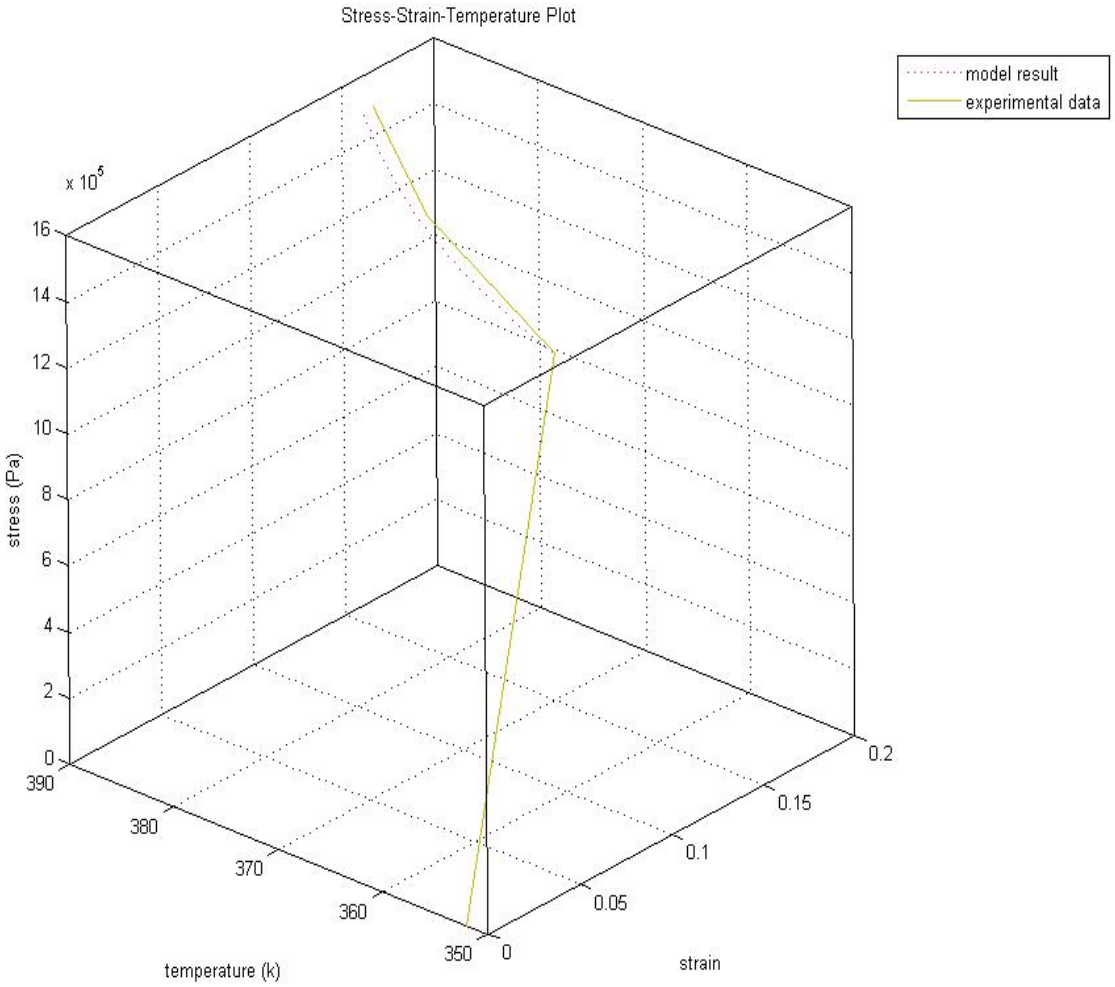


Fig. 22 .Comparison of model response with experimental result for a specified loading path.

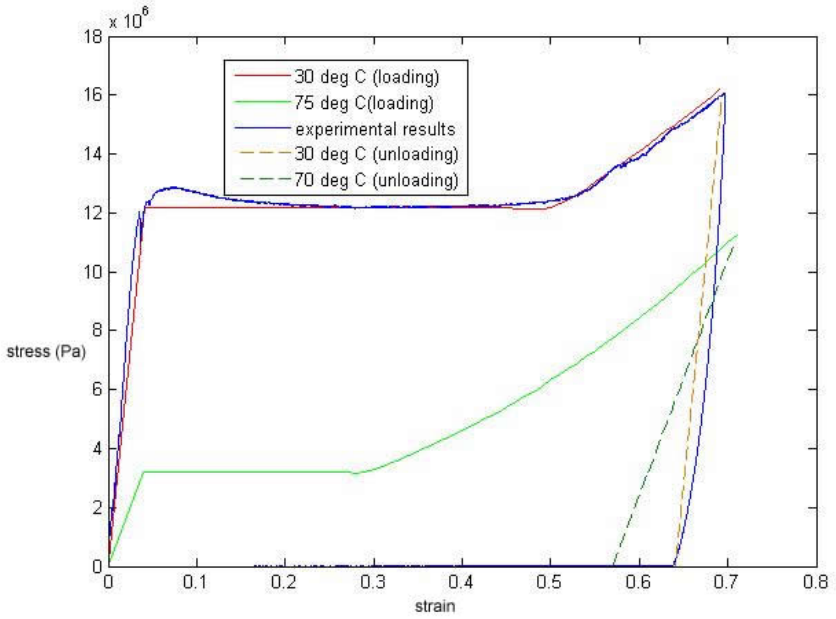


Fig. 23. Comparison of model response to loading and unloading paths

The results from this work are going to be used by Dr. S Bechtel and co-workers to develop a three dimensional model, which in addition to the fiber drawing process design, will help to increase the efficiency of the current fiber drawing processes. Numerical simulations can be performed with the use to methods like the Finite Element Method to understand to develop a better understanding of the design of fiber drawing.

# REFERENCES


[1] Bechtel SE, Vohra S and Jacob KI. Polymer 2001;42:2045-2059.

[2] Bechtel SE, Vohra S and Jacob KI. Polym Eng and Sci 2004;44(2):312-330.

[3] Bechtel SE, Vohra S and Jacob KI. Textile Res. J 2002;72(9):769-776.

[4] Buckley, CP and Jones, DC. Polymer 1995;41:2183–2201.

[5] Boyce MC, Socrate S and Llana PG. Polymer 2002;41:2183-2201.

[6] Argon AS. Phil. Mag 1973;28 (4): 839-865.

[7] Simpson P. Global Trends in Fiber Prices, Production and Consumption and Prices, March 2006 ed; Wilmslow, UK: Textiles Intelligence, 2006

[8] Herman MF. Encyclopedia of Polymer Science and Technology; New York: Wiley, 2002.

[9] Makradi A, Ahzi S, Gregory RV, Edie DD. Mechanics of Material 2002;35:1139-1148.

[10] Rajagopal KR, Kannan K and Rao IJ. J. Rheol. 2002;46:977-999.

[11] Zaroulis JS, Boyce MC. Polymer 1997;38:1303-1315.

[12] Jacob KI, Hsiao B, Bechtel S and Stein R. NTC Project: M01-GT04 2004. Spring House, PA: National Textile Center, 2004.

[13] Garmston S. World Synthetic Fibers Supply/Demand Report. PCI Fibers: Sussex, 1999.

[14] Callister WD. Material Science and Engineering- An Introduction, 2nd ed. New York: Wiley, 1992.

[15] McCrum NG, Buckley CP, Bucknall CB. Principles of Polymer Engineering 2 nd ed. New York: Oxford University Press,1997.

[16] Thompson AB. J Polym Sci 1959;35:741-760.

[17] Misra A and Stein RS. J Polym Sci 1979;17:235- 257.

[18] Gorlier, E, Haudin, JM, Billon N. Polymer 2001;42:9541–9549.

[19] Jabarin SA. Polym Eng and Sci 1992;32(18):1341-1349.

[20] Bensberg A. Continuum Mech. Thermodyn. 2003;15:409–423.

[21] Tobushi H, Ito N, Takata K and Hayashi S. Mater Sci Forum 1999;327-328:343-346.

[22] Chaari F, Chaouche M and Doucet J. Polymer 2003;44:473-479.

[23] Ward IM and Sweeney J. An Introduction to the Mechanical Properties of Solid Polymers. - 2nd ed. New York: Wiley, 2004.

[24] Brown N and Ward IM. Polymer Sci., A-2 1968;6:607-620.

[25] Kratochv´ıl J, M´alek J, Rajagopal KR and Srinivasa AR. Z. angew. Math. Phys. 2004;55:500-518.

[26] Khan AS and Huang S. Continuum Theory of Plasticity. New York: Wiley, 1995.

[27] Truesdell C, Noll W. The Non-Linear Field Theories of Mechanics.- Handbuch der Physik, Vol. III/3. Berlin: Springer,1965.

[28] Rajagopal KR and Srinivasa AR. Intern J Plast 1996;13:1-35.

# VITA


| | |
|---|---|
| Name: | Seemant Yadav |
| Address: | Dept. of Mechanical Engineering<br>C/o Dr. Arun Srinivasa<br>Texas A&M University,<br>College Station,<br>Texas 77843, USA. |
| Date of birth: | March 30, 1978. |


Education:

| | |
|---|---|
| 2003-2006 | Texas A&M University<br>Master of Science<br>Mechanical Engineering |
| 1996-2000 | Shri Govindram Seksaria Institute of Technology and Science,<br>Indore, India.<br>Bachelor of Engineering,<br>Mechanical Engineering |